Chemical Engineering Journal 277 (2015) 86–96

Contents lists available at ScienceDirect

Chemical Engineering Journal

journal homepage: www.elsevier.com/locate/cej

Enhancement of a solar photo-Fenton reaction by using ferrioxalate complexes for the treatment of a synthetic cotton-textile dyeing wastewater

Lucila I. Doumic [a,b,c], Petrick A. Soares [a], María A. Ayude [b], Miryan Cassanello [c], Rui A.R. Boaventura [a], Vítor J.P. Vilar [a,*]

[a] LSRE – Laboratory of Separation and Reaction Engineering, Associate Laboratory LSRE/LCM, Departamento de Engenharia Química, Faculdade de Engenharia da Universidade do Porto, Rua Dr. Roberto Frias, 4200-465 Porto, Portugal
[b] División Catalizadores y Superficies, Instituto de Investigaciones en Ciencia y Tecnología de Materiales – INTEMA, Departamento de Ingeniería Química, Universidad Nacional de Mar del Plata, J.B. Justo 4302, 7600 Mar del Plata, Argentina
[c] Laboratorio de Reactores y Sistemas para la Industria – LARSI, Departamento Industrias, Facultad Ciencias Exactas y Naturales, Universidad de Buenos Aires, Intendente Güiraldes 2620, C1428BGA Buenos Aires, Argentina

HIGHLIGHTS

- Strategies for the treatment of a cotton-textile dyeing wastewater are examined.
- Photo Fenton (PF) treatment leads to insoluble ferric–organic complexes.
- PF/Ferrioxalate remarkably improves wastewater mineralization rate.
- The suitability of combining biological and PF/Ferrioxalate processes is evaluated.

GRAPHICAL ABSTRACT

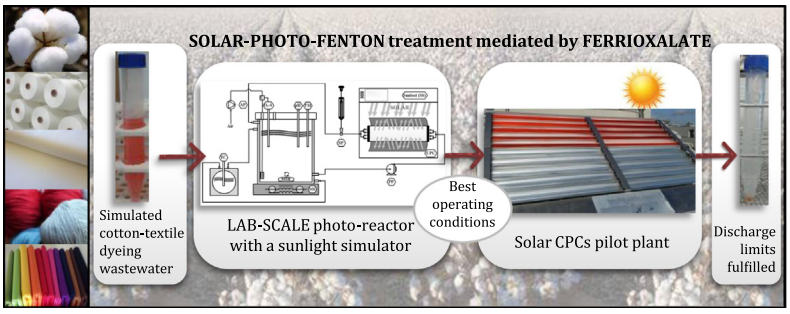

ARTICLE INFO

Article history:
Received 8 December 2014
Received in revised form 16 March 2015
Accepted 12 April 2015
Available online 18 April 2015

Keywords:
Cotton-textile dyeing wastewater
Dyes
Auxiliary products
Solar photo-Fenton
Ferrioxalate complexes

ABSTRACT

Biological, photo-Fenton (PF) and photo-Fenton mediated by ferrioxalate complexes (PF/Ferrioxalate) processes were examined for the degradation of a synthetic cotton-textile dyeing wastewater. Aerobic biological treatment had a negligible effect on discolouration whereas total organic content decreased mainly due to the biodegradation of acetic acid initially present in the wastewater. PF process yielded a fast and pronounced dissolved organic carbon concentration decay, mostly associated to the abrupt precipitation of Fe(III)–organic complexes. The addition of oxalic acid limited iron precipitation, allowing mineralization of most organic contaminants. The influence of the different dyes and main dyeing auxiliary constituents of the synthetic textile wastewater on the PF and the PF/Ferrioxalate efficiency was systematically analysed. The suitability of combining PF/Ferrioxalate with conventional biological processes as a pre and/or post treatment was evaluated.

This study highlights the potential of PF/Ferrioxalate reaction to mineralize the synthetic cotton-textile wastewater under appropriate experimental conditions, the best being: $[Fe^{3+}] = 40\ mg\ L^{-1}$, iron/oxalate molar ratio = 1:3, pH = 4.0 and $[H_2O_2] = 50–100\ (1.5–2.9)\ mg\ L^{-1}$ ($mmol\ L^{-1}$). At these conditions, the PF/Ferrioxalate treatment was carried out under natural sunlight in a pilot plant equipped with compound parabolic collectors.

* Corresponding author. Tel.: +351 918257824; fax: +351 225081674.
E-mail address: vilar@fe.up.pt (V.J.P. Vilar).

http://dx.doi.org/10.1016/j.cej.2015.04.074
1385-8947/

1. Introduction

The textile dyeing industry consumes large quantities of water and produces large volumes of wastewater [1]. Textile wastewater is heavily coloured and exhibit high salts content and biological recalcitrant character [2,3]. Therefore, development of robust and complete textile wastewater treatment methods is imperative for preserving the environment. Many chemical and physical processes have been proposed for the removal of dyes from wastewater, such as adsorption, coagulation, activated sludge treatment and oxidation by ozone or hypochlorite. These methods can be expensive and, in some cases, they may not eliminate the colour completely [4].

Recently, Advanced Oxidation Processes (AOPs) have emerged as an effective alternative to conventional methods. AOPs are characterized by the production of highly reactive radicals ($HO^{\cdot}$), which are able to degrade most of the recalcitrant organic pollutants due to their high oxidative capacity. Among the AOPs, the photo-Fenton (PF) process carried out under solar radiation as UV–Vis photon source for enhancing the $HO^{\cdot}$ generation is a potentially low cost technique [5,6]. However, application of this process for treating textile wastewater presents some drawbacks: (i) the coloured compounds reduce light penetration; (ii) textile wastewater is generally alkaline and PF works efficiently under acid conditions, to avoid iron precipitation and promote the pre-eminence of the photoactive ferric ion–water complex ($FeOH^{2+}$) species in solution [7]; (iii) ferric–organics complexes can be formed, limiting the photo-reduction of Fe^{3+} and thus decreasing the generation of radicals; (iv) the high content of inorganic ions (Cl^{-}, SO_4^{2-}, CO_3^{-}) induces the hydroxyl radicals scavenger reactions and the formation of inorganic ion–ferric complexes, which again decreases the rate of hydroxyl radicals generation [8–10].

To overcome these drawbacks, the addition of oxalic acid to PF treatment has been proposed [7,11,12]. PF mediated by ferrioxalate (PF/Ferrioxalate) offers further advantages over the conventional PF process. Ferrioxalate complexes provide much higher quantum yields, accelerating the regeneration of ferrous iron and therefore producing a higher amount of $HO^{\cdot}$ radicals; then, solar light is more efficiently used [13]. Ferrioxalate complexes reduce the formation of stable complexes between ferric ions and organic species present in wastewater. Moreover, in the presence of ferrioxalate, iron precipitation is inhibited even at near neutral pH (5–6) [7,14].

The application of a solar photo-Fenton reaction mediated by ferrioxalate complexes to different contaminants and wastewaters from various industrial sources has been recently reported. This treatment showed to be effective in the degradation of pure aqueous solutions contaminated with diclofenac [15], sulfamethoxazole and trimethoprim [16] at low iron concentrations and near neutral pH conditions. Monteagudo et al. [17] also showed the effectiveness of the photo-Fenton reaction mediated by ferrioxalate on the treatment of a real winery wastewater generated during the cleaning of winemaking facilities and equipment. Duran et al. [18] demonstrated that under certain conditions, the synergism between the photo-Fenton process and the ferrioxalate photochemistry was 22.9%, considering the treatment of a wastewater from a beverage industry. Recently, Soares et al. [19] evaluated different photo-Fenton-iron(III)–organic ligands complexes systems in the treatment of a synthetic acrylic-textile wastewater (mainly composed of a basic azo dye, and commercial auxiliary products such as, an Sera®Con N-VS, Sera® Tard A-AS, sodium sulphate, Sera®Sperce M-IW, Sera®Lube M-CF). The best results were obtained with the photo-Fenton reaction mediated by ferrioxalate. It is important to remark that the presence of specific auxiliary products, characterizing different types of textile wastewater, significantly and distinctly affect the applied Fenton and photo-Fenton processes. In this work, their influence is disclosed by comparing the process performance when applied to the synthetic cotton-dyeing wastewater and to isolated dyes and auxiliary products solutions. Moreover, the precipitation of Fe(III)–organic matter complexes generated in the photo-Fenton treatment is particularly examined.

Operating costs of the PF/Ferrioxalate process, mainly related to energy and reagents consumption, are higher than those of biological treatments. From an economic point of view, an effective treatment of recalcitrant wastewater may require a combination of processes, such as biological and advanced oxidation processes [6,20–23]. Refractory wastewater can be chemically pre-treated to increase biodegradability before being subjected to a conventional biological treatment. Alternatively, a biological pre-treatment can remove the biodegradable pollutants, therefore reducing the required amount of reagents in the subsequent oxidation process [6,21].

This research focuses on defining the best treatment strategy for a simulated/synthetic cotton-textile dyeing wastewater to accomplish the discharge limits established by Portuguese regulations. The viability of the PF and the PF/Ferrioxalate treatments using a photocatalytic tubular reactor irradiated with simulated solar radiation was particularly evaluated. The efficiency of the PF/Ferrioxalate process was evaluated under different iron concentrations, pH values and H_2O_2 availability. Operating conditions leading to the best performance were selected to carry out a solar-photo-Fenton/Ferrioxalate assay in a pilot plant equipped with compound parabolic collectors (CPCs). The extent of oxidation was assessed by analysing colour, organic matter content in terms of dissolved organic carbon (DOC), chemical oxygen demand (COD), 5 days biochemical oxygen demand (BOD_5), and biodegradability (Zahn Wellens test, BOD_5/COD ratio, carbon oxidation state (COS) and low-molecular-weight carboxylic acids content). Finally, the suitability of coupling biological with advanced oxidation processes was evaluated and discussed.

2. Experimental methodology

2.1. Preparation of the synthetic wastewater

The simulated cotton-textile wastewater was prepared by mixing the dyes (Procion Deep Red H-EXL gran and Procion Yellow H-EXL gran) and the auxiliary products, according to the information provided by the textile dyeing company Erfoc-Acabamentos Têxteis S.A. (Famalicão, Portugal). The concentration of each component in the final effluent was estimated taking into account the percentage of fixation of each compound on cotton fibres. This wastewater is assumed to be representative of the liquid effluent taken from the supernatant of a sedimentation tank. Samples of dyes and dyeing auxiliary products were kindly supplied by the above mentioned company and by DyStar Anilinas Têxteis, Unip Ltd (Porto, Portugal). Table 1 lists the dyes and auxiliary products used, their function and its contribution to DOC content on final wastewater. The biodegradable acetic acid (HAc) represents 40% of the total DOC content.

The characteristics of the simulated cotton textile dyeing wastewater are provided in Table 2. The synthetic wastewater has a low-moderate organic load. It presents a basic pH of 11.5 and a red-orange colour with a maximum absorbance peak at 478 nm. When acidified, the wastewater acquires a defined red colour, and the peak shifts to 518 nm. Wastewater colour remains visible after a dilution 1:40. The BOD_5/COD ratio of the synthetic effluent is relatively high (0.43); the Zahn–Wellens test indicates 56% of biodegradability after 28 days.

Table 1
Dyes and auxiliary products present in synthetic cotton-textile wastewater.

Dyeing product	Dyeing stage	Function	Chemical characteristic	Wastewater characteristics	
				Concentration	DOC (mg C L^{-1})
Procion Yellow H-EXL	Dyeing	Dyeing	Reactive azo dye	0.006 g L^{-1}	4.0
Procion Deep Red H-EXL gran	Dyeing	Dyeing	Reactive azo dye	0.04 g L^{-1}	12.5
Mouillant BG/JT	Fibre preparation	Anti-oil	Composition based in aliphatic ethoxylates	0.09 mL L^{-1}	10.8
Anticassure BG/BD	Fibre preparation	Anti-crease	Acrylamide aqueous solution	0.06 mL L^{-1}	0
Sodium hydroxide 50% (w/v)	Fibre preparation	Alkaline system	Base	0.57 mL L^{-1}	0
Hydrogen peroxide 200 vol.	Fibre preparation	Oxidizing the dye	Oxidant reagent	0.18 mL L^{-1}	0
Acetic acid	Fibre preparation	Acid generator	Acid	0.11 mL L^{-1}	45.2
Zerox	Fibre preparation	Hydrogen peroxide neutralizer	Catalase	0.08 mL L^{-1}	0
Enzyme BG/FB	Fibre preparation	Bleaching	Fungal cellulase	0.05 mL L^{-1}	2.8
Sequion M150	Dyeing	Water corrector	Composed by phosphonates/carboxylates	0.14 mL L^{-1}	33.6
Sodium chloride	Dyeing	Electrolyte	Electrolyte	1.16 g L^{-1}	0
Sodium carbonate	Dyeing	Alkaline system	Base	2.6 g L^{-1}	0
Sandozin NRW LIQ ALT C	Washing	Detergent	Polyethylene glycol isotridecyl ether	0.12 mL L^{-1}	5.1

Table 2
Simulated wastewater characterization.

Parameter	Units	Value
pH	Sorensen scale	11.5 (11.9)*
Alkalinity	g $CaCO_3$ L^{-1}	4.1
Conductivity	mS cm^{-1}	21.9
COD	mg O_2 L^{-1}	346 (226)*
BOD_5	mg O_2 L^{-1}	150 (40)*
BOD_5/COD	–	0.43 (0.19)*
DOC	mg C L^{-1}	110 (65)*
Zahn–Wellens biodegradability	%	56 (21)
Absorbance at 254 nm	–	1.262
Absorbance at λ_{max} −478 nm	–	0.525
Visible colour after dilution 1:40	–	visible
Acetic acid	mg L^{-1}	113
Sulphate	mg SO_4^{2-} L^{-1}	6.2
Chloride	g Cl^- L^{-1}	0.7
Phosphate	mg P-PO_4^{3-} L^{-1}	0.26
Sodium	g Na^+ L^{-1}	2.1
Potassium	mg K^+ L^{-1}	10
Magnesium	mg Mg^{2+} L^{-1}	29
Calcium	mg Ca^{2+} L^{-1}	170
Total nitrogen	mg N L^{-1}	10.0
Nitrate	mg N-NO_3^- L^{-1}	4.9
Nitrite	mg N-NO_2^- L^{-1}	4.9
Total suspended solids	mg TSS L^{-1}	73
Volatile suspended solids	mg VSS L^{-1}	52

* Values within brackets correspond to wastewater prepared without addition of acetic acid (HAc).

2.2. Reagents

All chemicals used were analytical grade without further purification. Ultrapure and deionized water used were produced by a Millipore® system (Direct-Q model) and a reverse osmosis system (Panice®), respectively.

2.3. Experimental set-up

2.3.1. Lab-scale photo-reactor prototype

Photo-Fenton runs were carried out in a lab-scale photo-reactor equipped with a sunlight simulator. The experimental set-up consisted in: (i) a stirred glass vessel (1.5 L capacity) surrounded by a cooling jacket coupled to a thermostatic bath (Lab. Companion, model RW-0525G); (ii) a solar radiation simulator (ATLAS, model SUNTEST XLS+) with 1100 cm^2 of exposition area, a 1700 W air-cooled xenon arc lamp, a daylight filter and quartz filter with IR coating; (iii) a compound parabolic collector (CPC) with 0.023 m^2 of illuminated area with anodized aluminium reflectors and a borosilicate tube (Schott–Duran type 3.3, Germany, cut-off at 280 nm, 46.4 mm internal diameter, 160 mm length and 1.8 mm thickness); (iv) a peristaltic pump (Ismatec, model Ecoline VC-380 II) and (v) a pH and temperature meter (VWR symphony – SB90M5). A schematic representation of the experimental set-up has been published by Soares et al. [24]. UV irradiance (280–400 nm) was measured by a broadband UV radiometer (Kipp & Zonen B.V., model CUV5) placed at the level of the photo-reactor center, inside the sunlight simulator. In order to record the incident UV irradiance (W_{UV} m^{-2}), a radiometer was plugged into a handheld display unit (Kipp & Zonen B.V., model Meteon).

2.3.2. Solar CPC pilot plant

An experiment, using the operating conditions that led to the best results in the lab-scale photo-reactor, was carried out under sunlight in a 50-L pilot plant. The pilot plant, operated in batch mode, consisted of CPCs (2.19 m^2), a polypropylene storage conic tank (50 L), a recirculation pump (ARGAL, model TMB), a flow meter (Stübe, model DFM 165-350), polypropylene valves (FIP) and connecting tubing. The solar collector comprises ten borosilicate glass tubes (Schott–Duran type 3.3, Germany, cut-off at 280 nm, 46.4 mm internal diameter, 1500 mm length and 1.8 mm thickness) connected in series by polypropylene junctions, mounted on a fixed platform tilted 41° (local latitude), toward the south. Solar UV irradiance was measured by a global UV radiometer (ACADUS 85-PLS) mounted on the pilot plant at the same angle, which provides data in terms of incident W_{UV} m^{-2}. Accumulated UV energy ($Q_{UV,n}$ kJ L^{-1}) received during the time interval Δt on any surface inside the reactor at the same position regarding the sun, expressed per unit of reactor volume, can be calculated by the Eq. (1).

$$Q_{UV,n} = Q_{UV,n-1} + \Delta t_n \overline{UV}_{G,n} \frac{A_r}{1000 \times V_t}; \quad \Delta t_n = t_n - t_{n-1} \tag{1}$$

where t_n (s) is the time corresponding to the instant at which the n-water sample was taken, V_t (L) is the total reactor volume, A_r (m^2) is the illuminated collector surface area, and $\overline{UV}_{G,n}$ (W_{UV} m^{-2}) is the average solar ultraviolet irradiation measured during the period Δt_n (s).

2.3.3. Biological system

Biological treatments were carried out at ambient temperature in a glass vessel (1.5 L capacity) equipped with a magnetic stirrer. An air pump was used to supply oxygen to the activated sludge, through air diffusers located on the bottom of the reactor.

2.4. Experimental procedure

2.4.1. Oxidation experiments

Experiments in the lab-scale photo-reactor were performed using 1.0 L of the simulated textile wastewater, which was

pumped to the CPC unit and homogenized in the darkness by recirculation at 1.15 L min^{-1}. The illuminated reactor volume is 0.27 L, resulting in an illumination time of 0.24 min and a darkness time of 0.63 min. Solution temperature was maintained at 30 °C. The pH of the reaction solution was adjusted to the desired value by using sulfuric acid or sodium hydroxide. The pH was controlled along the whole experiment to keep an almost constant value. For PF runs, pH was adjusted to 2.8; then, the desired amount of solid $FeSO_4{\cdot}7H_2O$ was added. For PF/Ferrioxalate, oxalic acid was added (iron/oxalate molar ratio 1:3), and pH was adjusted to the desired value before adding $FeCl_3{\cdot}6H_2O$ to achieve the desired concentration. Samples were taken after Fenton's reactants addition to evaluate initial conditions. The SUNTEST was turned on, and the irradiance was set at 500 W m^{-2} (41.3 W_{UV} m^{-2}). The first dose of hydrogen peroxide was added and samples were taken at pre-defined times to evaluate the degradation process. Along the reaction course, H_2O_2 concentration was kept within the desired range: 50–100 (1.5–2.9), 100–200 (2.9–5.9) or 200–300 (5.9–8.8) mg L^{-1} (mmol L^{-1}), by replenishing the consumed amount. PF and PF/Ferrioxalate runs using solutions of each wastewater component were also carried out following the above procedure.

For the solar-photo-Fenton/Ferrioxalate reaction test in the solar CPCs pilot plant, 40 L of wastewater was added to the storage tank of the CPC unit (2.19 m^2 of illuminated area) and it was recirculated at 20 L min^{-1}. Best experimental conditions found at the lab-scale reactor were selected for the pilot plant experiment. Wastewater was homogenized during 15 min in the darkness; immediately after, a first control sample was taken for further characterization. Oxalic acid (iron/oxalate molar ratio of 1:3) was then added and pH was adjusted to 4.0 using H_2SO_4 (a second sample was taken after 15 min to confirm the pH). Afterwards, ferric chloride (40 mg Fe^{3+} L^{-1}) was added and homogenized for 15 min before taking the third sample for iron concentration control. Finally, H_2O_2 was added, the CPCs were uncovered and the reaction started. Samples were then taken at different time intervals to evaluate the degradation process. The pH was adjusted along the whole experiment to keep an almost constant value. H_2O_2 concentration was maintained within 1.5–2.9 mmol L^{-1} by replenishing the consumed amount.

2.4.2. Biological experiments

For each test, 1.0 L of solution was placed into the reactor and pH was adjusted with H_2SO_4 or NaOH to a value near 7 (±0.5). Mineral nutrients (KH_2PO_4, K_2HPO_4, Na_2HPO_4, NH_4Cl, $CaCl_2$, $MgSO_4$ and $FeCl_3$) and activated sludge from a municipal wastewater treatment plant (WWTP) were added into the glass vessel. The amount of centrifuged-activated sludge was estimated taking into account the ratio between inoculum and dissolved organic carbon established in Oecd [25]. Stirring and air supply started and after 15 min the first sample was taken. Further samples were then taken at different time intervals to evaluate the biological degradation process. The pH and dissolved oxygen concentration were controlled within the range of 6.5–7.5 and 1.0–3.0 mg O_2 L^{-1}, respectively.

2.5. Analytical determinations and methods

Total dissolved iron concentration (TDI) was measured by a spectrometric method using 1,10-phenanthroline, according to ISO 6332 [26]. The vanadate method [27] was employed to evaluate H_2O_2 concentration along the experiments. Colour after 1:40 dilution was visually assessed. A UNICAM Helios spectrophotometer was used to obtain the UV–Vis spectrums between 200 and 800 nm. The absorbance at 518 nm was measured along the reaction to determine the degree of colour removal. Absorbances at 510 nm (phenanthroline method) and 450 nm (vanadate method) were also monitored. Since the textile wastewater absorbs at these wavelengths, measurements were corrected by the absorbance of a blank/control sample measured at the corresponding wavelengths. Carboxylic acids were measured using an ion-exclusion HPLC (VWR Hitachi ELITE LaChrom) fitted with a RezexTM ROA-Organic Acid H+(8%) 300 × 7.8 mm (Phenomenex) column. It was operated at 298 K and in isocratic mode using 0.005 N H_2SO_4 at a flow rate of 0.5 mL min^{-1} as mobile phase. Samples of 10 μL were injected and the DAD (L-2455) was set at λ = 210 nm. The method allowed the simultaneous detection of 17 carboxylic acids: oxalic, tartronic, maleic, citric, oxamic, tartaric, malic, malonic, glycolic, succinic, shikimic, formic, acetic, glutaric, fumaric, propionic and acrylic. Inorganic ions were quantified by ion chromatography (Dionex ICS-2100 and Dionex DX-120 for anions and cations, respectively) using a Dionex Ionpac (columns AS9-HC/CS12A 4 mm × 250 mm; suppressor ASRS®300/CSRS®300 4 mm, anions/cations). The programme for anions/cations determination comprises a 12 min run with 30 mM NaOH/20 mM methanesulfonic acid at a flow rate of 1.5/1.0 mL min^{-1}. Samples were filtered through 0.45 μm Nylon membrane filters before analysis.

Dissolved organic carbon (DOC) was measured by a TC-TOC-TN analyser (Shimadzu, model TOC-VCSN) equipped with ASI-V auto sampler (Shimadzu, model TOC-VCSN). Total dissolved nitrogen was measured in the same TC-TOC-TN analyser coupled with a TNM-1 unit (Shimadzu, model TOC-VCSN), by thermal decomposition and NO detection by the chemiluminescence method. Alkalinity was evaluated by titration with H_2SO_4 at pH 4.5 – Method 2320 D [28]. pH and temperature were measured with a pH meter VWR symphony-SB90M5, and conductivity was measured using a pH meter HANNA HI 4522. Chemical oxygen demand (COD) was determined with Merck Spectroquant kits (ref: 1.14541.0001).

The carbon oxidation state (COS) parameter, indicative of the oxidation degree and the oxidative process effectiveness [29], was calculated as:

$$COS = 4 - 1.5\frac{COD}{DOC_0} \quad (2)$$

where DOC_0 (mg C L^{-1}) is the initial dissolved organic carbon concentration, and COD (mg O_2 L^{-1}) is the chemical oxygen demand at time *t*.

Biochemical oxygen demand (BOD_5) was determined according to OECD-301F test using an OxiTop (manometric respirometry), as described in Standard Methods [28]. Total suspended solids (TSS) and Volatile suspended solids (VSS) were quantified according to Standard Methods [28]. Before the analysis (except TSS, VSS and COD), all samples were centrifuged in a HIMAC CT 6E centrifuge at 4000 rpm for 5 min. Before biological tests and COD measurements, remnant H_2O_2 was removed: pH was adjusted to 6.5–7.5 and a small volume (0.4 mL L^{-1}) of a 0.1 g L^{-1} catalase solution (2500 U mg^{-1} bovine liver) was added. COD measurements were corrected considering a blank solution containing the same amount of catalase added to the samples.

The 28 days Zahn–Wellens biodegradability test was performed according to EC protocol, Directive 88/303/EEC [25]. 240 mL of the samples obtained along the solar-photo-Fenton/Ferrioxalate reaction were put in an open glass vessel, magnetically stirred and kept in the dark at 25 °C. Centrifuged activated sludge from a municipal WWTP and mineral nutrients (KH_2PO_4, K_2HPO_4, Na_2HPO_4, NH_4Cl, $CaCl_2$, $MgSO_4$ and $FeCl_3$) were added to the samples. The added amount of centrifuged-activated sludge was estimated taking into account the ratio between inoculum and dissolved organic carbon of each pre-treated sample, as established in OECD [25]. Control and blank experiments with mineral nutrients and activated sludge were carried out using glucose (which is highly biodegradable) as carbon source and pure distilled water, with and without

the addition of catalase, respectively. The percentage of biodegradation (D_t) was determined by the following equation:

$$D_t = \left[1 - \frac{C_t - C_B}{C_A - C_{BA}}\right] \times 100 \quad (3)$$

where C_t and C_B are DOC (mg C L^{-1}) measured at the sampling time t in sample and in blank, respectively; C_A and C_{BA} are DOC (mg C L^{-1}) measured 3 h after the activated sludge addition in sample and in blank, respectively.

3. Results and discussion

3.1. Biological treatment

The colour remains practically unchanged after biological treatment of the synthetic textile wastewater. DOC profile can be found in Fig. SM-1 (Supplementary material). Residual DOC is reduced up to 51 mg C L^{-1} after 30 h approximately. According to ion-exclusion HPLC analyses, the initially existing carboxylic acids are biologically oxidized.

Additionally, an acetic acid (HAc) solution (45 mg C L^{-1}) was subjected to the same biological treatment and similar DOC removal rate was observed (see Fig. SM-1). This confirms that mainly acetic acid is being biologically consumed while treating the synthetic textile wastewater. Even though 20 h are needed to remove HAc when the activated sludge is used for the first time, half the time is enough when using a wastewater-adapted activated sludge (data not shown).

After the biological pre-treatment, wastewater fulfils the established limits for most of the parameters (pH, COD and BOD_5), according to Ordinance 423/97 for discharge of textile wastewater in Portugal. However, as no colour reduction is attained (i.e. colour after 1:40 dilution is still visible) further treatment is required and a chemical oxidation stage can be a good option.

3.2. Photo-Fenton reactions

Fig. 1 shows outcomes of the simulated wastewater photo-Fenton treatment using $[Fe^{2+}] = 60$ mg L^{-1}, $[H_2O_2] = 2.9$–5.9 mmol L^{-1} and $I = 41.3$ W_{UV} m^{-2} at pH = 2.8 and $T = 30$ °C. An initially steep DOC decay (36%) and fast discolouration (99% within 6 min ≈ 0.36 kJ_{UV} L^{-1}) is attained. Mineralization proceeds at a much lower rate, likely associated to: (i) a low amount of dissolved iron, not enough to suppress the inner filter effects (competitive absorption of photons by other light absorbing species in the wastewater); (ii) too slow photo-reduction via a ligand-to-metal charge mechanism occurring on the surface of the precipitated iron. Furthermore, the DOC remaining after the initial decay is mostly associated to the acetic acid in the synthetic textile wastewater. Acetic acid molecule is very recalcitrant to hydroxyl radicals attack and the soluble ferric–acetate complexes have low photoactivity [30,31], thus explaining the slow DOC degradation rate observed in the second part of the treatment. In addition, a red precipitate was detected after centrifugation, suggesting formation of complexes between ferric ions and dyes and/or dyeing auxiliary products.

To confirm the existence of insoluble iron–organics complexes, ferrous or ferric iron salts were added under stirring conditions to the synthetic wastewater at room temperature and pH 2.8, in absence of hydrogen peroxide and radiation. Subsequent variation of DOC and total dissolved iron (TDI) concentrations with time are shown in Fig. 2. Neither iron precipitation nor DOC decay takes place in the presence of 60 mg L^{-1} of ferrous ion. However, the same concentration of ferric ion results in a fast DOC decay (31.5 mg C L^{-1}) accompanied by a decrease of 40 mg L^{-1} in TDI concentration. These outcomes evidence the formation of highly stable complexes between ferric ions and dyes and/or dyeing auxiliary products, which may precipitate. The extent of precipitation diminishes with the decrease of initial ferric concentration, being almost negligible for 10 mg Fe^{3+} L^{-1}.

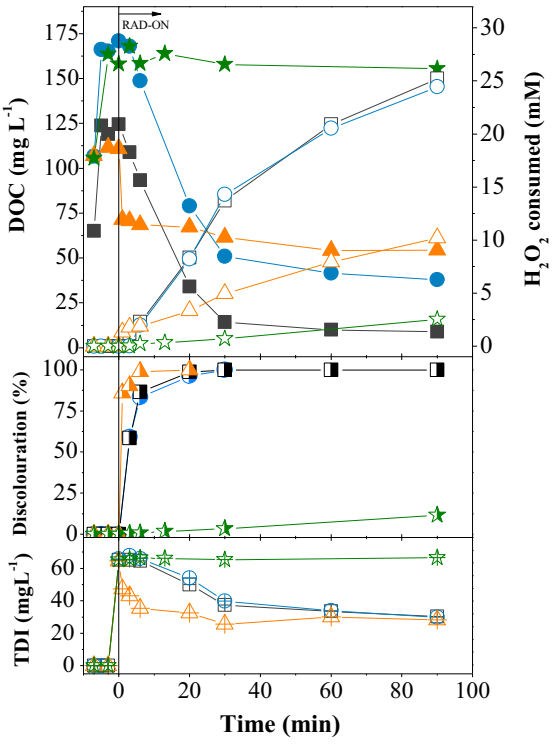

Fig. 1. Simulated textile wastewater treatment strategies examined. Solid symbols: DOC; open symbols: consumed H_2O_2; half solid symbols: % discolouration; cross symbols: total dissolved iron (TDI). (▲,△,◭,◬) Photo-Fenton; (●,○,◑,⊕) photo-Fenton/Ferrioxalate; (■,□,◧,⊞) photo-Fenton/Ferrioxalate using wastewater *without* acetic acid; (★,☆,✱,✲) Fenton/Ferrioxalate. Operating conditions: pH = 2.8; $T = 30$ °C; $[Fe] = 60$ mg L^{-1}; $[H_2O_2] = 2.9$–5.9 mmol L^{-1}; $I = 41.3$ W_{UV} m^{-2}.

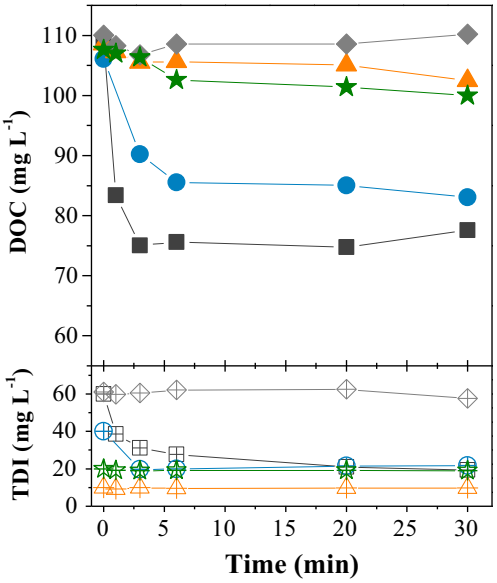

Fig. 2. Evolution of DOC and total dissolved iron concentrations (TDI) after addition of different ferrous and ferric iron concentrations to the simulated cotton textile wastewater in the absence of H_2O_2 and light at pH = 2.8 and room temperature ($T \approx 22$ °C). (●,○) $[Fe^{2+}]_0 = 60$ mg L^{-1}; (■,⊞) $[Fe^{3+}]_0 = 60$ mg L^{-1}; (●,⊕) $[Fe^{3+}]_0 = 40$ mg L^{-1}; (★,✲) $[Fe^{3+}]_0 = 20$ mg L^{-1}; (▲,◬) $[Fe^{3+}]_0 = 10$ mg L^{-1}.

Thus, deep mineralization via photo-Fenton process of the tested wastewater is impeded by precipitation of iron–organics insoluble complexes. These outcomes also suggest that insoluble iron organic complexes would be also promoted by Fenton reaction, since ferrous ion is oxidised by hydrogen peroxide to yield ferric ions. Rodrigues et al. [32], have recently stated that photo-Fenton process applied to synthetic cotton dyeing wastewater permits reaching high efficiencies in discolouration and considerable organic compounds mineralization. These authors observed similar trends as those described above within the first minutes (colour removal ≅99% and DOC removal ≅40%); however, the formation of ferric–DOC complexes and precipitates was not assessed. It should be underlined that under these reaction conditions, a decrease in DOC does not guarantee mineralization.

The influence of wastewater components on the PF process and their contribution to iron precipitation is described hereafter. Dyes and auxiliary compounds containing a measurable DOC content were exposed to PF reaction. HAc is excluded since its degradation is negligible under the studied conditions [30].

Fig. 3 shows that Sequion M150, the reactive dyes Procion Deep Red H-EXL gran and Procion Yellow H-EXL, and Sandozin NRW LIQ ALT C are responsible for iron precipitation. A sudden decrease in DOC and TDI concentrations is initially observed, indicating the formation of insoluble ferric–organic matter complexes. In contrast, when a solution of Mouillant BG/JT solution is treated, TDI concentration remains constant and DOC progressively decreases, indicating that PF degradation can proceed.

Colour removal from textile wastewater by chemical coagulation/flocculation using ferric ions as a coagulant has been extensively reported [33,34]. The COD removal depends on pH and on the type of dye [35]. To our knowledge, contributions dealing specifically with homogeneous Fenton and/or photo-Fenton oxidation of Procion Deep Red H-EXL gran or Procion Yellow H-EXL solutions have not reported precipitation of ferric–dye complexes [36–38].

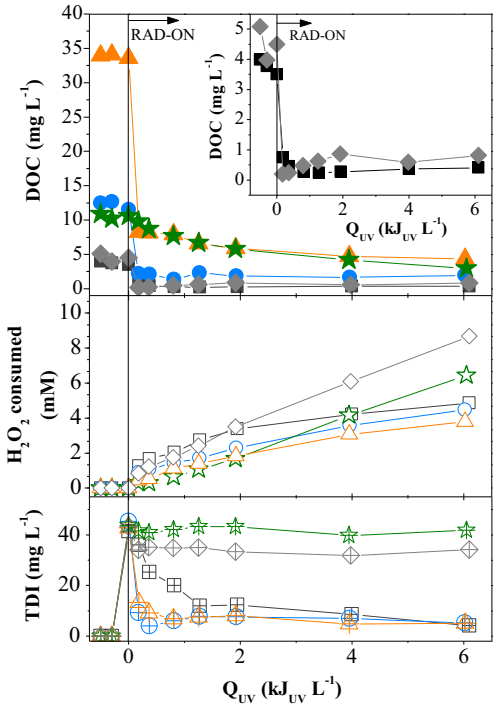

Fig. 3. PF reaction applied to the individual solutions of auxiliary dyeing products and dyes. Evolution of DOC (solid symbols), consumed H_2O_2 (open symbols) and total dissolved iron – TDI (cross symbols). Operating conditions: pH = 2.8; T = 30 °C; $[Fe^{2+}]$ = 40 mg L^{-1}; $[H_2O_2]$ = 1.5–2.9 mmol L^{-1}; I = 41.3 W m^{-2}. (■,□,⊞) Procion Yellow H-EXL; (●,○,⊕) Procion Deep Red H-EXL gran; (▲,△,≙) Sequion M150; (★,☆,✲) Mouillant BG/JT; (◆,◇,✣) Sandozin NRW LIQ ALT C.

Sandozin NRW LIQ ALT C is basically a non-ionic surfactant; the coagulation of similar compounds after the addition of ferric salts has been previously reported [39].

The formation of iron-Sequion M150 complex may be explained by the presence of phosphonate groups in Sequion M150's chemical structure, which form stable complexes with ferric ions. Sequion M150 is frequently used as a chelating agent of heavy metals in many applications, e.g., in pulp, paper and textile industries [40].

3.3. Photo-Fenton process mediated by ferrioxalate complexes

The addition of chelating agents to generate more stable ferric complexes than those formed with the wastewater components appears as an alternative to prevent precipitation and promote oxidation. Several researchers have reported the chemistry and photochemistry of ferric and ferrous complexes in the presence of oxalic acid [41,42]. Oxalic acid forms strong complexes with ferric ions inhibiting the undesired interactions with other organic and/or inorganic compounds [7,36]. Its presence also accelerates the process providing a more efficient pathway to regenerate ferrous from ferric iron [7,43,44].

Enhancement of the photo-Fenton reaction through the use of oxalic acid while treating the synthetic cotton textile dyeing wastewater is described below. Oxalic to iron ratio is set to 1:3 to promote formation of the most stable complex ($Fe(C_2O_4)_3^{3-}$) [12,13,41]. A lower oxalate concentration would result scarce, slowing down the ferrous iron regeneration rate, whereas an excess would act as hydroxyl radicals' scavenger.

Addition of oxalic acid substantially improves the efficiency of photo-Fenton reaction (see Fig. 1). In these experiments, no sludge formation is observed; i.e., no precipitation of organics occurs. Wastewater is completely discoloured within 30 min (1.9 kJ_{UV} L^{-1}) with $[Fe^{3+}]$ = 60 mg L^{-1}, $[H_2O_2]$ = 2.9–5.9 mmol L^{-1} and I = 41.3 W_{UV} m^{-2} at pH = 2.8 and T = 30 °C. Compared to results attained with the traditional photo-Fenton process, a slightly slower discolouration rate and a higher hydrogen peroxide consumption rate are observed.

Although initial DOC concentration is larger when oxalic acid is added, ferrioxalate complexes are easily photodecarboxylated under UV–visible radiation. PF/Ferrioxalate delays iron precipitation; TDI decreases less abruptly than in the PF process as the ferrioxalate complex is degraded. After 40 min of reaction, no residual oxalic acid is detected. Carboxylic acids analysis indicates that residual DOC is mainly related to the initial HAc content (not shown), which could be removed through a biological degradation process, as it was demonstrated in Section 3.2.

The wastewater after a biological pre-treatment can be emulated by preparing the simulated wastewater without including the acetic acid. The outcomes attained in a PF/Ferrioxalate experiment using the wastewater prepared without HAc are also included in Fig. 1 for comparison purposes. It arises that initial HAc content has negligible effect on wastewater degradation rate during PF/Ferrioxalate treatment. Residual DOC, lower than 10 mg C L^{-1}, is associated to remnant low-molecular-weight carboxylic acids: mainly acetic acid and, to a lesser extent, tartaric, formic, succinic and fumaric acids (data not shown). H_2O_2 consumption is not affected by the initial HAc content.

Since acetic acid can be effectively degraded by a biological pre-treatment, and has negligible effect on PF/Ferrioxalate process, this compound is not included in the simulated textile wastewater for subsequent experiments.

Finally, a control experiment in the darkness is performed to assess the contribution of Fenton/Ferrioxalate oxidation (see

Fig. 1). Under these conditions, DOC removal and hydrogen peroxide consumption are negligible. TDI remains constant since ferrioxalate complexes are not degraded in the absence of radiation. Similar results were obtained by Arslan et al. [13], who reported negligible degradation under dark Fe(III)–oxalate-Fenton reaction of a simulated dye-house effluent (containing Procion H reactive dyes and their corresponding auxiliary chemicals).

Outcomes of the PF/Ferrioxalate treatment of dyes and the main dyeing auxiliary components are shown in Fig. 4. Whatever the component, almost complete DOC removal is achieved after an accumulated UV energy of 1.3 $kJ_{UV}\ L^{-1}$; the small residual DOC mainly corresponds to formed acetic acid.

For Procion Yellow H-EXL, Procion Deep Red H-EXL gran, Mouillant BG/JT and Sandozin NRW LIQ ALT C, TDI remains almost constant, even once the oxalic acid is totally depleted. However, while treating a Sequion M150 solution, iron precipitation is observed. In addition, phosphate concentration increases up to 1.3 $kJ_{UV}\ L^{-1}$ of accumulated energy (data not shown), suggesting that phosphonate groups forming Sequion M150 chemical structure are being oxidized to phosphate ions by hydroxyl radicals [45]. At 1.3 $kJ_{UV}\ L^{-1}$ of accumulated energy, oxalate concentration is almost depleted and phosphate concentration starts decreasing due to precipitation of insoluble ferric–phosphate complexes [46]. Thus, Sequion M150 may be responsible for iron precipitation observed in the PF/Ferrioxalate treatment of the synthetic textile wastewater.

3.4. Effect of different reaction variables on photo-Fenton/Ferrioxalate process

The addition of oxalic acid allows achieving total discolouration and substantial mineralization of the simulated textile wastewater. Pursuing the optimization of the process, the influences of iron concentration, H_2O_2 availability and pH on the simulated wastewater PF/Ferrioxalate treatment are examined.

3.4.1. Effect of iron concentration

Results from the PF/Ferrioxalate treatment of the simulated cotton-textile wastewater prepared without HAc using different iron concentrations (20–60 mg $Fe^{3+}\ L^{-1}$) are shown in Fig. 5. Discolouration rate and the degree of mineralization substantially improve when iron concentration is increased from 20 to 40 mg L^{-1}. A further increase in iron concentration improves only marginally DOC removal and substantially promotes H_2O_2 consumption. Discolouration rate is not further enhanced. Hence, an iron concentration of 40 mg $Fe^{3+}\ L^{-1}$ is enough to maximize the absorption of UV–visible photons, overcoming the presence of other light-absorbing species in solution (e.g., dyes).

3.4.2. Effect of H_2O_2 concentration

The available concentration of hydrogen peroxide plays a very important role in the PF process, basically because it is largely responsible for the generation of the hydroxyl radicals. Results from PF/Ferrioxalate experiments with different oxidant availability are depicted in Fig. 6. Hydrogen peroxide concentration is kept always within a given range (1.5–2.9, 2.9–5.9 or 5.9–8.8 mmol L^{-1}) by adding successive doses of H_2O_2.

Among the studied ranges, H_2O_2 availability does not modify significantly either the DOC removal profile or the TDI concentration along the reaction. No effect is observed in discolouration profile (data not shown); 99% of colour removal is achieved after 1.2 $kJ_{UV}\ L^{-1}$ of accumulated energy. Although more hydroxyl radicals would be expected since oxidant decomposition is enhanced, an increase in H_2O_2 availability favours parasitic reactions and

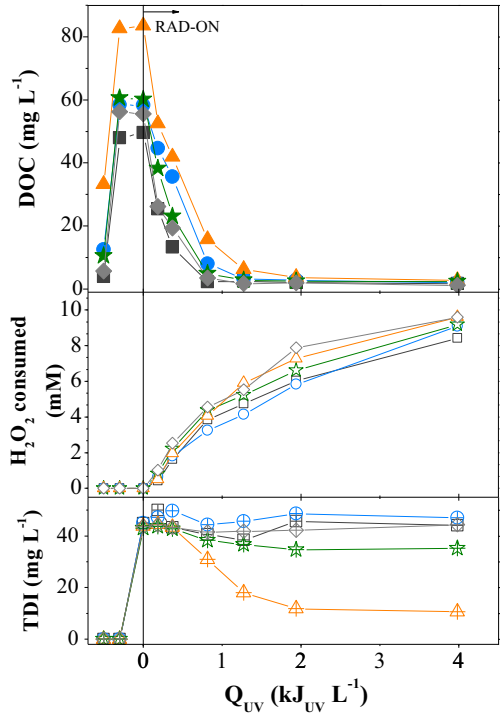

Fig. 4. PF/Ferrioxalate process applied to the individual solutions of auxiliary dyeing products and dyes. Evolution of DOC (solid symbols), consumed H_2O_2 (open symbols) and total dissolved iron – TDI (cross symbols) under the following operating conditions: pH = 2.8; T = 30 °C; $[Fe^{3+}]$ = 40 mg L^{-1}; $[H_2O_2]$ = 1.5–2.9 mmol L^{-1}; I = 41.3 W m^{-2}; iron/oxalate molar ratio 1:3. (■,□,⊞) Procion Yellow H-EXL; (●,○,⊕) Procion Deep Red H-EXL gran; (▲,△,≙) Sequion M150; (★,☆,✲) Mouillant BG/JT; (◉, ○, ⊕) Sandozin NRW LIQ ALT C.

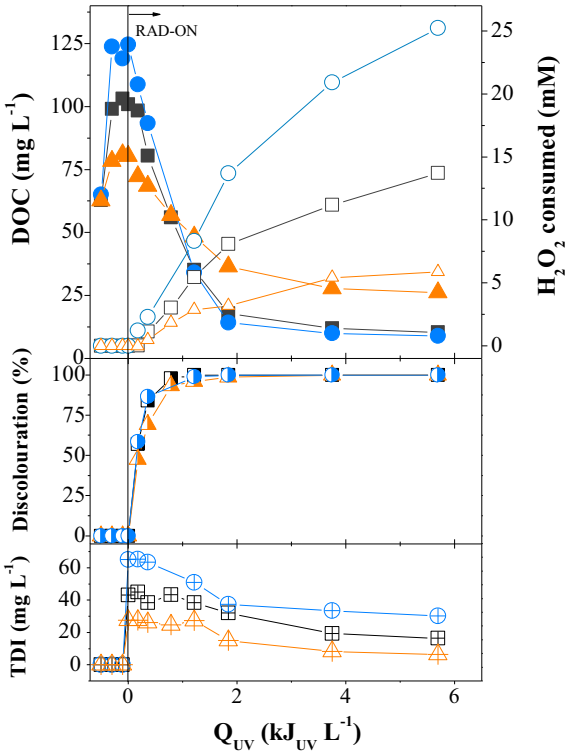

Fig. 5. PF/Ferrioxalate reactions carried out with different iron concentrations. Solid symbols: DOC; open symbols: consumed H_2O_2; half solid symbols: % discolouration; cross symbols: total dissolved iron (TDI). (▲,△,◭,≙) $[Fe^{3+}]$ = 20 mg L^{-1}; (■,□,◧,⊞) $[Fe^{3+}]$ = 40 mg L^{-1}; (●,○,◑,⊕) $[Fe^{3+}]$ = 60 mg L^{-1}. Operating conditions: pH = 2.8; T = 30 °C; $[H_2O_2]$ = 2.9–5.9 mmol L^{-1}; I = 41.3 W m^{-2}; iron/oxalate molar ratio 1:3.

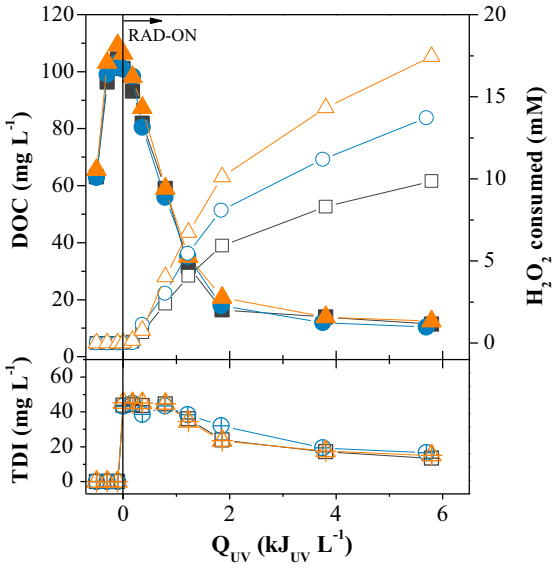

Fig. 6. Evolution of DOC (solid symbols), consumed H_2O_2 (open symbols) and total dissolved iron – TDI (cross symbols) for the PF/Ferrioxalate reaction of simulated wastewater without HAc using different hydrogen peroxide concentrations. Operating conditions: pH = 2.8; T = 30 °C; $[Fe^{3+}]$ = 40 mg L^{-1}; iron/oxalate molar ratio 1:3; I = 41.3 W m^{-2}. (■,□,⊞) $[H_2O_2]$ = 1.5–2.9 mmol L^{-1}; (●,○,⊕) $[H_2O_2]$ = 2.9–5.9 mmol L^{-1}; (▲,△,⧋) $[H_2O_2]$ = 5.9–8.8 mmol L^{-1}.

the efficiency for radical generation decreases. Therefore, the lower H_2O_2 concentration range ($[H_2O_2]$ = 1.5–2.9 mmol L^{-1}) is selected for further experiments.

3.4.3. Effect of pH

One of the critical operating parameters of the photo-Fenton process is pH, since it highly affects the generation of hydroxyl radicals and the nature of the iron species in solution. The need for acidification in the PF process represents one of its major disadvantages. Not only additional cost is generated by the consumption of reagents needed for acidification and subsequent neutralization, but also treated wastewater's salt load increases. Several researchers proposed that acidification could be circumvented in the presence of complexing agents [14,47,48]. In this sense, the performance of PF/Ferrioxalate is examined at different pHs (2.8, 3.5, 4.0, 5.0 and 6.0) using 40 mg L^{-1} of Fe^{3+} and $[H_2O_2]$ = 1.5–2.9 mmol L^{-1}. Fig. 7 shows the evolution of DOC, the fraction of DOC related to oxalate and TDI concentration; whereas Fig. SM-2 (Supplementary material) presents the discolouration and H_2O_2 consumption profiles (DOC profile is included for the sake of comparison). Results indicate that the PF/Ferrioxalate system is able to work efficiently up to pH 4.0. When pH is further increased, a decrease in discolouration, DOC abatement and oxidant consumption is observed. This experimental observation can be explained by the speciation of Fe^{3+} as a function of pH.

Fig. 8 shows the iron speciation diagram in presence of oxalic acid, for a ferric iron concentration of 40 mg L^{-1} (T = 30 °C and ionic strength = 0.13 M). The diagram is obtained using the chemical equilibrium modelling system MINEQL+ [49], taking into account the oxalic acid speciation, iron–sulphate, iron–chloride and iron–oxalate complexes equilibrium reactions (Table SM-1 of Supplementary material). The equilibrium constants taken from literature are corrected to zero ionic strength using the Davies Equation [50]. Fig. 8 evidences the reason why the addition of oxalic acid to the reaction media extends the pH range suitable for the process application, since precipitation of $Fe(OH)_3$ is delayed until pH = 4.8. Between pH = 2.8 and 4.8, iron remains in solution as $Fe(C_2O_4)_3^{3-}$ and $Fe(C_2O_4)_2^-$. pH higher than 4.8 reduces the

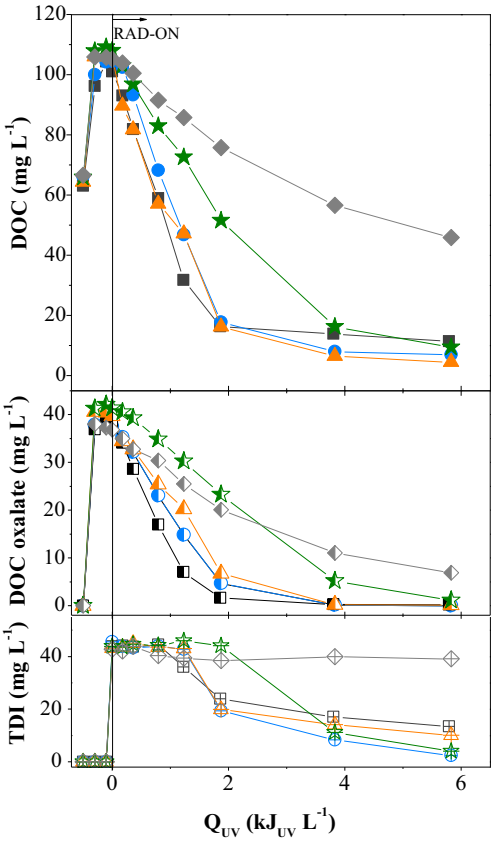

Fig. 7. Effect of pH on the PF/Ferrioxalate process applied to the simulated wastewater without HAc. Operating conditions: T = 30 °C; $[Fe^{3+}]$ = 40 mg L^{-1}; $[H_2O_2]$ = 1.5–2.9 mmol L^{-1}; iron/oxalate molar ratio 1:3; I = 41.3 W m^{-2}. (■,⊞,◧) pH = 2.8; (●,⊕,◐) pH = 3.5; (▲,◭,◮) pH = 4; (★,✯,★) pH = 5; (◆,◈,◇) pH = 6.

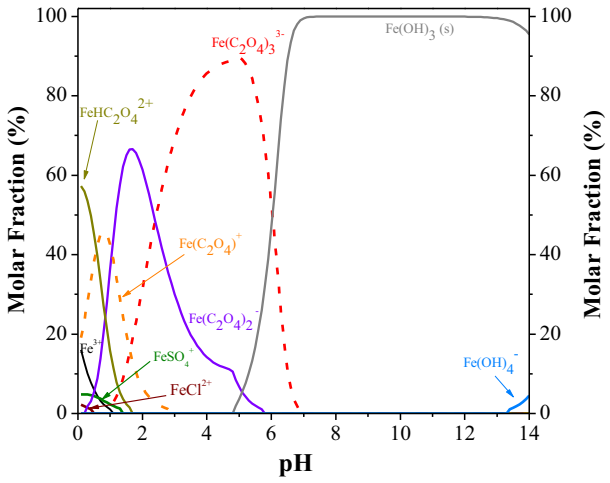

Fig. 8. Speciation diagram of ferric complexes as a function of pH for a solution containing 7.16×10^{-4} M of Fe^{3+} (40 mg Fe^{3+} L^{-1}), 2.15×10^{-3} M (189 mg $C_2O_4^{2-}$ L^{-1}) of oxalic acid, 2.14×10^{-2} M of Cl^- and 2.5×10^{-2} M of SO_4^{2-}. Ionic strength = 0.13 M and temperature = 30 °C.

efficiency of the process due to the diminished photoactivity of the ferrioxalate complexes [7,44,51], since longer times are necessary to achieve total photodecarboxylation of oxalic acid. Fig. 7 shows that almost no mineralization of the textile wastewater occurred at the highest examined pH. The DOC abatement is mainly associated to the photodecarboxylation of ferrioxalate complexes. However, even after almost total consumption of oxalic

acid, TDI concentration remains approximately constant (in the absence of oxalic acid, iron starts to precipitate at pH higher than 2.9), which indicates that iron species form soluble complexes with the organic pollutants present in the textile wastewater for pH values higher than 6.0. The slow mineralization rate can be mainly associated to the low photoactivity of those soluble iron–organic pollutants complexes, principally for the highest pH values.

3.5. Solar photo-Fenton process mediated by ferrioxalate complexes at pilot scale

Experimental conditions leading to the best results for lab-scale conditions (pH = 4.0, $[Fe^{3+}]$ = 40 mg L^{-1}, iron/oxalate molar ratio = 1:3 and $[H_2O_2]$ = 1.5–2.9 mmol L^{-1}) are selected to carry out the solar-photo-Fenton/Ferrioxalate treatment of the simulated wastewater in the solar CPCs pilot plant, under natural sunlight ($\bar{I}$ = 24 W_{UV} m^{-2}; $\bar{T}$ = 25 °C).

Evolution of colour removal, consumed H_2O_2, DOC, COD, TDI and oxalic acid concentrations are represented as a function of the accumulated energy in Fig. 9. Additional information, such as the evolution of BOD_5/COD ratio, carbon oxidation state (COS), fraction of DOC related to low-molecular-weight carboxylate anions (LMCA/DOC ratio) and carboxylic acids concentrations can be found in Fig. SM-3 (Supplementary material).

Solar-photo-Fenton/Ferrioxalate process at pilot scale proves to be a very good treatment method for the simulated cotton-textile wastewater. Almost complete discolouration is achieved, which is the main objective of the PF/Ferrioxalate stage. Fig. 9 shows that colour quickly decreases until 0.6 kJ_{UV} L^{-1} and then proceeds at a slower rate, whereas DOC and COD are gradually removed along the treatment.

Fig. SM-4 (Supplementary material) illustrates the evolution of colour in undiluted samples and in samples diluted by a factor 40. Colour at 1:40 dilution is no longer visible by eye after 3.2 kJ_{UV} L^{-1} of accumulated energy (Sample S_7). At this point, 98.3% of colour removal is achieved and 11.2 mM of H_2O_2 is consumed. Residual DOC and COD are 14 and 57 mg L^{-1}, respectively. This high level of organic matter oxidation correlates well with the COS parameter shown in Fig. SM-3, which increases from −1.1 to +2.7, suggesting that the wastewater organic compounds are mineralized or transformed into highly oxidized intermediates.

The fraction of DOC that corresponds to low-molecular-weight carboxylate anions (LMCA/DOC ratio), without including the carbon of oxalic acid added (COAA), increases from null to 79% after an accumulated energy of 3.2 kJ_{UV} L^{-1} (corresponding to 3.6, 2.2, 0.7 and 4.7 mg C L^{-1} of tartrate, malonate, formate and acetate, respectively). The LMCA/DOC ratio with COAA is 36% in sample S_2, and the difference between LMCA/DOC with and without COAA decreases as ferrioxalate complexes are photodecarboxylated, as shown in Fig. SM-3.

When oxalic acid concentration falls below ~30 mg L^{-1} (1.9 kJ_{UV} L^{-1} of accumulated energy), TDI concentration decreases, mainly due to iron precipitation with phosphate ions.

Table SM-2 (Supplementary material) shows the evolution of the inorganic anions along the treatment. Phosphate, sulphate, chloride, nitrite and nitrate anions were detected. Phosphate ions profile exhibits a maximum at 1.9 kJ_{UV} L^{-1}, evidencing the gradual generation of phosphate and its subsequent precipitation with iron. Sulphate concentration increases initially from 6.2 mg SO_4^{2-} L^{-1} to 2.3 g SO_4^{2-} L^{-1} after acidification, and continues growing up to 2.5 g SO_4^{2-} L^{-1} due to the gradual H_2SO_4 addition to keep the pH value constant. Chloride ion concentration increases from 687 mg Cl^- L^{-1} to 760 mg Cl^- L^{-1}, once ferric chloride is added.

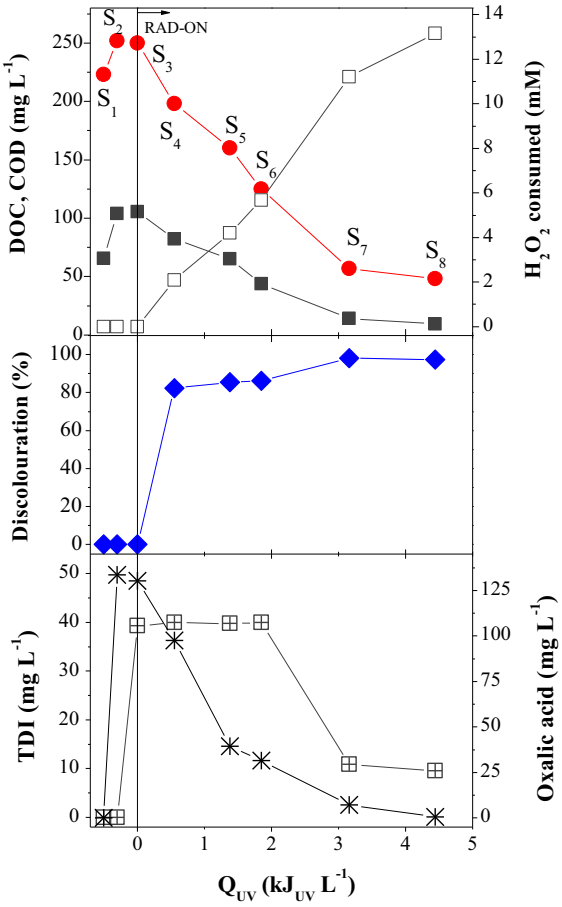

Fig. 9. Pilot scale solar photo-Fenton/Ferrioxalate treatment of the synthetic cotton-textile dyeing wastewater without acetic acid at pH = 4, $[Fe^{3+}]$ = 40 mg L^{-1}, iron/oxalate molar ratio 1:3, $[H_2O_2]$ = 1.5–2.9 mmol L^{-1}, $\bar{I}$ = 24 W m^{-2} and $\bar{T}$ = 25 °C. Profiles corresponding to: (■) DOC; (●) COD; (□) consumed H_2O_2; (◆) discolouration; (⊞) total dissolved iron (TDI) and (✳) oxalic acid.

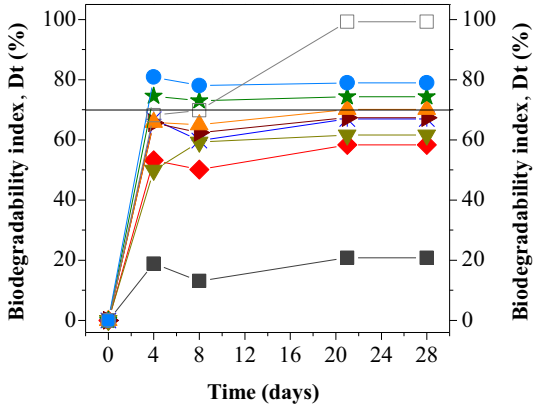

Fig. 10. Results from the Zahn Wellens test for samples taken along the solar photo-Fenton/Ferrioxalate reaction. (■) S_1: DOC = 65.5 mg L^{-1}; (◆) S_2: DOC = 104.2 mg L^{-1}; (▼) S_3: DOC = 105.5 mg L^{-1}; (✳) S_4: DOC = 82.0 mg L^{-1}; (▶) S_5: DOC = 65.3 mg L^{-1}; (▲) S_6: DOC = 43.8 mg L^{-1}; (★) S_7: DOC = 14.1 mg L^{-1}; (●) S_8: DOC = 8.2 mg L^{-1}; (□) reference, DOC = 100 mg L^{-1}.

The organic nitrogen can be released in ionic and gaseous forms, such as nitrate, nitrite, ammonia, molecular nitrogen, dinitrogen monoxide, nitrogen monoxide [52]. Total nitrogen (TN) evolution is included in Fig. SM-5 (Supplementary material). TN concentration quickly decreases from 10 to 5 mg N L^{-1} after acidification and then, slowly decays to 4 mg N L^{-1} along the PF treatment. The initial drop

may be explained considering the acidic reduction of nitrite ions leading to NO and other nitrogen oxides [53]. Then, gaseous products are progressively formed. Nitrate ion concentration is practically constant and no ammonia is detected along the reaction time.

Results obtained with the Zahn–Wellens test carried out for samples taken along the PF/Ferrioxalate reaction are shown in Fig. 10. Wastewater without acetic acid exhibits a low biodegradability index, D_t (21% after 28 days), which is significantly improved by the PF/Ferrioxalate treatment. Once wastewater fulfils the discharge requirements after the PF/Ferrioxalate stage (Sample S_7), biodegradability index reaches values higher than 70% and the BOD_5/COD ratio is above 0.4 (threshold value).

As a whole, an acceptable degree of discolouration and biodegradability is achieved after applying a coupled biological and solar PF/Ferrioxalate treatment.

4. Conclusions

The degradation of a simulated textile wastewater is considered by different advanced oxidation and biological processes. Biological degradation is not efficient since discolouration is not achieved. The photo-Fenton processes do not represent a convenient technique to oxidize the tested simulated cotton-textile dyeing wastewater. Insoluble and low photoactive ferric complexes are formed with the used reactive dyes and the auxiliary dyeing products Sequion M150 and Sandozin NRW LIQ ALT C, leading to iron precipitation at low pH.

However, the PF/Ferrioxalate process leads to a real mineralization of this textile wastewater. Best results for the lab-scale tests are obtained using: $[Fe^{3+}] = 40\ mg\ L^{-1}$, iron/oxalate molar ratio = 1:3, pH = 4.0 and $[H_2O_2] = 1.5–2.9\ mmol\ L^{-1}$. At these conditions, the acetic acid-free simulated effluent subjected to a PF/Ferrioxalate process in a solar CPCs pilot plant accomplishes the discharge limits established by Portuguese regulations. After $3.2\ kJ_{UV}\ L^{-1}$ of accumulated energy, 98.3% of colour removal, 11.2 mM of H_2O_2 consumption, $14.2\ mg\ C\ L^{-1}$ of residual DOC and $57\ mg\ O_2\ L^{-1}$ of remnant COD are achieved. The PF/Ferrioxalate treatment significantly enhances the wastewater biodegradability. Iron precipitation is evidenced when more than 70% of the initially added oxalic acid is already photodecarboxylated. Precipitates are likely related to oxidation products of the phosphonate groups present in Sequion M150 chemical structure, forming insoluble ferric–phosphate complexes. The viability and effectiveness of coupled biological and solar PF/Ferrioxalate treatment to mineralize this textile wastewater is demonstrated.

Acknowledgements

This work was partially supported by project UID/EQU/50020/2013, financed by FEDER through COMPETE – Programa Operacional Factores de Competitividade, by FCT – Fundação para a Ciência e a Tecnologia and by QREN, ON2 and FEDER (Project NORTE-07-0162-FEDER-000050). P.A. Soares acknowledges his Ph.D. fellowship (BEX 5512-10-7) supported by CAPES. V.J.P. Vilar acknowledges the FCT Investigator 2013 Programme (IF/01501/2013). L.I. Doumic acknowledges CONICET, the European Commission and the Erasmus Mundus Action 2-ARCOIRIS scholarship for their support. M.A. Ayude and M.C. Cassanello are members of CONICET (Argentina) and thank P.M. Haure for her valuable comments.

Appendix A. Supplementary data

Supplementary data associated with this article can be found, in the online version, at http://dx.doi.org/10.1016/j.cej.2015.04.074.

References

[1] V.M. Correia, T. Stephenson, S.J. Judd, Characterisation of textile wastewaters – a review, Environ. Technol. 15 (1994) 917–929.
[2] B.R. Babu, A.K. Parande, S. Raghu, T.P. Kumar, Cotton textile processing: waste generation and effluent treatment, J. Cotton Sci. 11 (2007) 141–153.
[3] T. Robinson, G. Mcmullan, R. Marchant, P. Nigam, Remediation of dyes in textile effluent: a critical review on current treatment technologies with a proposed alternative, Bioresour. Technol. 77 (2001) 247–255.
[4] I.K. Konstantinou, T.A. Albanis, TiO_2-assisted photocatalytic degradation of azo dyes in aqueous solution: kinetic and mechanistic investigations: a review, Appl. Catal., B 49 (2004) 1–14.
[5] D. Spuhler, J. Rengifo-Herrera, C. Pulgarin, The effect of Fe^{2+}, Fe^{3+}, H_2O_2 and the photo-Fenton reagent at near neutral pH on the solar disinfection (SODIS) at low temperatures of water containing *Escherichia coli* K12, Appl. Catal., B 96 (2010) 126–141.
[6] I. Oller, S. Malato, J.A. Sánchez-Pérez, Combination of advanced oxidation processes and biological treatments for wastewater decontamination – a review, Sci. Total Environ. 409 (2011) 4141–4166.
[7] S. Malato, P. Fernández-Ibáñez, M.I. Maldonado, J. Blanco, W. Gernjak, Decontamination and disinfection of water by solar photocatalysis: recent overview and trends, Catal. Today 147 (2009) 1–59.
[8] J. De Laat, G. Truong Le, B. Legube, A comparative study of the effects of chloride, sulfate and nitrate ions on the rates of decomposition of H_2O_2 and organic compounds by Fe(II)/H_2O_2 and Fe(III)/H_2O_2, Chemosphere 55 (2004) 715–723.
[9] A.J. Machulek, J.E.F. Moráles, C. Vautier-Gongo, C.A. Silverio, L.C. Friedrich, C.a.O. Nascimiento, M. González, F.H. Quina, Abatement of the inhibitory effect of chloride anions on the photo-Fenton process, Environ. Sci. Technol. 41 (2007) 8459–8463.
[10] A.N. IgnatEv, A.N. Pryakhin, V.V. Lunin, Mathematical simulation as a method to study the influence of oxygen, hydrogen peroxide, and phosphate and carbonate ions on the kinetics of ozone decomposition in aqueous solution, Russ. Chem. Bull. Int. Ed. 58 (2009) 1097–1105.
[11] R.G. Zepp, B.C. Faust, J. Holgné, Hydroxyl radical formation in aqueous reactions (pH 3–8) of iron(II) with hydrogen peroxide: the photo-Fenton reaction, Environ. Sci. Technol. 26 (1992) 313–319.
[12] J.J. Pignatello, E. Oliveros, A. Mackay, Advanced oxidation processes for organic contaminant destruction based on the fenton reaction and related chemistry, Crit. Rev. Environ. Sci. Technol. 36 (2006) 1–84.
[13] I. Arslan, I.A. Balcioglu, D.W. Bahnemann, Advanced chemical oxidation of reactive dyes in simulated dyehouse effluents by ferrioxalate-Fenton/UV-A and TiO_2/UV-A processes, Dyes Pigm. 47 (2000) 207–218.
[14] M. Vedrenne, R. Vasquez-Medrano, D. Prato-Garcia, B.A. Frontana-Uribe, M. Hernandez-Esparza, J.M. De Andrés, A ferrous oxalate mediated photo-Fenton system: toward an increased biodegradability of indigo dyed wastewaters, J. Hazard. Mater. 243 (2012) 292–301.
[15] B.M. Souza, M.W.C. Dezotti, R.A.R. Boaventura, V.J.P. Vilar, Intensification of a solar photo-Fenton reaction at near neutral pH with ferrioxalate complexes: a case study on diclofenac removal from aqueous solutions, Chem. Eng. J. 256 (2014) 448–457.
[16] I.N. Dias, B.S. Souza, J.H.O.S. Pereira, F.C. Moreira, M.W.C. Dezotti, R.a.R. Boaventura, V.J.P. Vilar, Enhancement of the photo-Fenton reaction at near neutral pH through the use of ferrioxalate complexes: a case study on trimethoprim and sulfamethoxazole antibiotics removal from aqueous solutions, Chem. Eng. J. 247 (2014) 302–313.
[17] J.M. Monteagudo, A. Durán, J.M. Corral, A. Carnicer, J.M. Frades, M.A. Alonso, Ferrioxalate-induced solar photo-Fenton system for the treatment of winery wastewaters, Chem. Eng. J. 181–182 (2012) 281–288.
[18] A. Durán, J.M. Monteagudo, J. Gil, A.J. Expósito, I. San Martín, Solar-photo-Fenton treatment of wastewater from the beverage industry: intensification with ferrioxalate, Chem. Eng. J. 270 (2015).
[19] P.A. Soares, M. Batalha, S.M.A. Guelli, U. Souza, R.A.R. Boaventura, V.J.P. Vilar, Enhancement of a solar photo-Fenton reaction with ferric-organic ligands for the treatment of acrylic-textile dyeing wastewater, J. Environ. Manage. 152 (2015) 120–131.
[20] J. Scott, D. Ollis, Integration of chemical and biological oxidation processes for water treatment: review and recommendations, Environ. Prog. 14 (1995) 88–102.
[21] V. Sarria, S. Parra, N. Adler, P. Péringer, N. Benitez, C. Pulgarin, Recent developments in the coupling of photoassisted and aerobic biological processes for the treatment of biorecalcitrant compounds, Catal. Today 76 (2002) 301–315.
[22] F. Feng, Z. Xu, X. Li, W. You, Y. Zhen, Advanced treatment of dyeing wastewater towards reuse by the combined Fenton oxidation and membrane bioreactor process, J. Environ. Sci. 22 (2010) 1657–1665.
[23] A. Cesaro, V. Naddeo, V. Belgiorno, Wastewater treatment by combination of advanced oxidation processes and conventional biological systems, J. Bioremed. Biodegrad. 4 (2013) 208.
[24] P. Soares, T.C.V. Silva, D. Manenti, S.a.G.U. Souza, R.R. Boaventura, V.P. Vilar, Insights into real cotton-textile dyeing wastewater treatment using solar advanced oxidation processes, Environ. Sci. Pollut. Res. 21 (2014) 932–945.
[25] OECD, OECD Guidelines for the Testing of Chemicals in Test No. 302B: Inherent Biodegradability: Zahn-Wellens/EMPA, OECD Publishing, 1992.

[26] ISO 6332:1988, Water Quality-Determination of Iron-Spectrometric Method Using 1,10-Phenanthroline, 1988.
[27] R.F.P. Nogueira, M.C. Oliveira, W.C. Paterlini, Simple and fast spectrophotometric determination of H_2O_2 in photo-Fenton reactions using metavanadate, Talanta 66 (2005) 86–91.
[28] L.S. Clesceri, A.E. Greenberg, A.D. Eaton, Standard Methods for Examination of Water & Wastewater, American Public Health Association (APHA), American Water Works Association (AWWA) & Water Environment Federation (WEF), 2005.
[29] A.M. Amat, A. Arques, F. Galindo, M.A. Miranda, L. Santos-Juanes, R.F. Vercher, R. Vicente, Acridine yellow as solar photocatalyst for enhancing biodegradability and eliminating ferulic acid as model pollutant, Appl. Catal., B 73 (2007) 220–226.
[30] E. Guinea, F. Centellas, J.A. Garrido, R.M. Rodríguez, C. Arias, P.L. Cabot, E. Brillas, Solar photoassisted anodic oxidation of carboxylic acids in presence of Fe^{3+} using a boron-doped diamond electrode, Appl. Catal., B 89 (2009) 459–468.
[31] E.M. Rodríguez, B. Núñez, G. Fernández, F.J. Beltrán, Effects of some carboxylic acids on the Fe(III)/UVA photocatalytic oxidation of muconic acid in water, Appl. Catal., B 89 (2009) 214–222.
[32] C.S.D. Rodrigues, L.M. Madeira, R.a.R. Boaventura, Optimization and economic analysis of textile wastewater treatment by photo-fenton process under artificial and simulated solar radiation, Ind. Eng. Chem. Res. 52 (2013) 13313–13324.
[33] H.R. Guendy, Treatment and reuse of wastewater in the textile industry by means of coagulation and adsorption techniques, J. Appl. Sci. Res. 6 (2010) 649–972.
[34] A.K. Verma, R.R. Dash, P. Bhunia, A review on chemical coagulation/flocculation technologies for removal of colour from textile wastewaters, J. Environ. Manage. 93 (2012) 154–168.
[35] T.H. Kim, C. Park, J. Yang, S. Kim, Comparison of disperse and reactive dye removals by chemical coagulation and Fenton oxidation, J. Hazard. Mater. 112 (2004) 95–103.
[36] A. Riga, K. Soutsas, K. Ntampegliotis, V. Karayannis, G. Papapolymerou, Effect of system parameters and of inorganic salts on the decolorization and degradation of Procion H-exl dyes. Comparison of H_2O_2/UV, Fenton, UV/Fenton, TiO_2/UV and TiO_2/UV/H_2O_2 processes, Desalination 211 (2007) 72–86.
[37] K. Ntampegliotis, A. Riga, V. Karayannis, V. Bontozoglou, G. Papapolymerou, Decolorization kinetics of Procion H-exl dyes from textile dyeing using Fenton-like reactions, J. Hazard. Mater. 136 (2006) 75–84.
[38] C.S.D. Rodrigues, L.M. Madeira, R.a.R. Boaventura, Optimization of the azo dye Procion Red H-EXL degradation by Fenton's reagent using experimental design, J. Hazard. Mater. 164 (2009) 987–994.
[39] A. Ayguna, T. Yilmaz, Improvement of coagulation–flocculation process for treatment of detergent wastewaters using coagulant aids, Int. J. Chem. Environ. Eng. 1 (2010) 97–101.
[40] B. Nowack, Environmental chemistry of phosphonates, Water Res. 37 (2003) 2533–2546.
[41] J.M. Monteagudo, A. Durán, M. Aguirre, I. San Martín, Photodegradation of Reactive Blue 4 solutions under ferrioxalate-assisted UV/solar photo-Fenton system with continuous addition of H_2O_2 and air injection, Chem. Eng. J. 162 (2010) 702–709.
[42] M.S. Lucas, J.A. Peres, Degradation of Reactive Black5 by Fenton/UV-C and ferrioxalate/H_2O_2/solar light processes, Dyes Pigm. 74 (2007) 622–629.
[43] H.-P. Cheng, Y.-H. Huang, C. Lee, Decolorization of reactive dye using a photo-ferrioxalate system with brick grain-supported iron oxide, J. Hazard. Mater. 188 (2011) 357–362.
[44] A. Safarzadeh-Amiri, J.R. Bolton, S.R. Cater, Ferrioxalate-mediated photodegradation of organic pollutants in contaminated water, Water Res. 31 (1997) 787–798.
[45] A. Aguila, K.E. O'shea, T. Tobien, K.D. Asmus, Reactions of hydroxyl radical with dimethyl methylphosphonate and diethyl methylphosphonate. a fundamental mechanistic study, J. Phys. Chem. A 105 (2001) 7834–7839.
[46] R.B. Wilhelmy, R.C. Patel, E. Matijevici, Thermodynamics and kinetics of aqueous ferric phosphate complex formation, Inorg. Chem. 24 (1985) 3290–3297.
[47] Y. Sun, J.J. Pignatello, Chemical treatment of pesticide wastes. Evaluation of iron(III) chelates for catalytic hydrogen peroxide oxidation of 2,4-D at circumneutral pH, J. Agric. Food Chem. 40 (1992) 322–327.
[48] J. Jeong, J. Yoon, PH effect on OH radical production in photo/ferrioxalate system, Water Res. 39 (2005) 2893–2900.
[49] W.D. Schecher, D.C. Mcavoy, MINEQL+: a chemical equilibrium modeling system, version 4.6 for windows, in: Environmental Research Software, Hallowell, Maine, United States, 2007.
[50] C. Sawyer, P. Mccarty, G. Parkin, Chemistry for Environmental Engineering and Science, McGraw-Hill Education, 2003.
[51] M.E. Balmer, B. Sulzberger, Atrazine degradation in irradiated iron/oxalate system: effects of pH and oxalate, Environ. Sci. Technol. 33 (1999) 2418–2424.
[52] P. Maletzky, R. Bauer, The Photo-Fenton method – degradation of nitrogen containing organic compounds, Chemosphere 37 (1998) 899–909.
[53] A.D. Ormerod, A.A. Shah, H. Li, N.B. Benjamin, G.P. Ferguson, C. Leifert, An observational prospective study of topical acidified nitrite for killing methicillin-resistant *Staphylococcus aureus* (MRSA) in contaminated wounds, BMC Res. Notes 4 (2011) 458.